PAPER *Special Section on Recent Technologies ot Microwave and Millimeter-Wave Devices*

Fiber-Optic Broadband Signal Distribution Link Based on a Millimeter-Wave Self-Heterodyne Transmission/Optical Remote Heterodyne Detection Technique

Yozo SHOJI[†a)], **Yoshihiro HASHIMOTO**[††], ***and*** **Hiroyo OGAWA**[†], ***Members***

SUMMARY A fiber-optic broadband signal distribution link based on a millimeter-wave self-heterodyne transmission/optical remote heterodyne detection technique was developed. To avoid having to use expensive optical and millimeter-wave devices to construct a frequency-stable fiber-optic millimeter-signal transmission system, a millimeter-wave self-heterodyne transmission technique was used, in which transmitted signals were generated by an optical remote heterodyne detection scheme. Theoretical discussion and experiments demonstrated that it is possible to construct an inexpensive millimeter-wave signal distribution link without the complexity or difficulties of a conventional link structure because applying the principle of the millimeter-wave self-heterodyne transmission technique enables the use of an unstable millimeter-wave carrier generated by heterodyning of two independently operating lasers. It was experimentally demonstrated that the proposed fiber-optic millimeter-wave link could successfully achieve bit-error-free transmission of a 156-Mb/s QPSK-formatted signal over a 10-km fiber link and a 5-m pseudo-air link.

key words: *millimeter-wave, optical remote heterodyne, self-heterodyne, optical SSB modulator*

1. Introduction

Interest in fiber-optic millimeter-wave links has been increasing, with proposed applications ranging from optical phased-array antenna feeders to fiber-optic remote antennas for fixed wireless access systems [1], [2].

A fiber-optic millimeter-wave link implemented using an optical intensity modulation/direct detection (IM/DD) technique is the most obvious system from the point of view of simplicity and signal transparency although this would require the development of a broadband extemal optical modulator (EOM) and photo-detector that could respond to millimeter-wave frequency and signal quality degrades due to fiber chromatic dispersion. However, a link implemented using optical remote heterodyne detection (RHD) [3] also has potential advantages because it is based on optical two-mode beating and is thus capable of generating extremely high frequency millimeter-waves from IF signal, although this would also require the development of a broadband photo-detector that could respond to these frequencies. An additional advantage of the RHD is that it provides a frequency-conversion function.

With advances in research on generating sub-millimeter or terahertz waves, the development of extremely broadband photonic devices has also made rapid progress in recent years. The development of a photo-detector with a bandwidth of more than 1 THz based on a uni-traveling-carrier photo diode (UTC-PD) was recently reported [5]. This means that using the principles of optical two-mode beating and broadband photo-detection easily generates sub-millimeter or terahertz waves.

In spite of the potential advantages of using RHD, however, when service operators look at constructing new signal transmission infrastructure based on fiber-optic links, the possibility of using optical RHD technology tends to be discounted due to its higher complexity and cost. The main reasons for this are that it requires two laser transmitters with slightly different wavelengths in which the phases of the two optical carriers must be strictly correlated [3], or a mode-locked dual-frequency laser transmitter [4]; the higher the target frequency, the more difficult it is to obtain a carrier that is sufficiently stable to carry the modulated signal.

In our research on a simple millimeter-wave link (not combined with fiber-optic) for use in the future, we discovered that using a millimeter-wave self-heterodyne transmission technique enables extremely frequency-stable signal transmission even when using a low-cost, unstable millimeter-wave oscillator [6] . From the theoretical viewpoint, the principle of this transmission technique is also effective when using an unstable millimeter-wave carrier generated by heterodyning two optical carriers, the phases of which are not correlated at all. Consequently, we consider that the complexity and cost of implementing fiber-optic millimeter-wave links could be greatly reduced with this technique even if we apply the RHD instead.

To create a cost-effective millimeter-wave/sub-millimeter-wave distribution system that could actually carry the modulated data, this paper proposes and demonstrates a fiber-optic broadband signal distribution link based on millimeter-wave self-heterodyne transmission over an optical remote heterodyne detection scheme, designed for use with a remote antenna system. The experiments in this paper demonstrate the scheme's operating principles and the practicality of using the 60-GHz frequency band. However, we believe this system could also be effectively applied in the near future to the use of sub-millimeter or terahertz waves

Manuscript received October 19, 2004.
Manuscript revised January 25, 2005.

[†]The authors are with National Institute of Information and Communications Technology, Incorporated Administrative Agency, Yokosuka-shi, 239-0847 Japan.
[††]The author is with Sumitomo Osaka Cement Co., Ltd., Funabashi-shi, 274-8601 Japan.
a) E-mail: y-shoji @ieee.org

DOI: 10.1093/ietele/e88-c.7.1465

for communication, that is, for carrying modulated signals.

Section 2 outlines the concept of a fiber-optic broadband signal distribution link with a remote antenna system and discusses the problems encountered in conventional approaches. Section 3 describes the basic system configuration and operating principles of our proposed link. Section 4 describes the experimental setup, and Sect. 5 presents the experimental results in terms of the millimeter-wave spectrum, phase-noise cancellation effect, received carrier-to-noise power ratio (CNR) performance, and bit-error-rate (BER) performance when a 156-Mbps QPSK signal was transmitted over our system.

2. System Concept and Discussion on Performance among IM/DD and RHD Techniques

Figure 1 illustrates the concept of using remote antenna systems to distribute broadband millimeter-wave signals for mobile terminals based on a fiber-optic link technique. The fiber-optic link is used to connect the base station (BS) and several remote antenna stations (RAS). Functions such as media access control, allocation of frequency channel, and modulation/demodulation, are installed in the BS and millimeter-wave signals are transmitted over optical fiber to the RAS, which are configured as simply as possible. The RAS basically detect the transmitted optical signals and convert them to the millimeter-wave signals for distribution via radio cells.

Although Fig. I illustrates the concept of a remote antenna system with a point-to-multipoint (P-MP) network topology from the viewpoint of practicality, this paper consistently discusses the fiber-optic link system with a point-to-point (P-P) network topology. However, if we try to provide simple broadcast-like signal distributing services, the use of simple passive optical networking technique, that is, merely power splitting of the transmitted optical signal from the BS, realizes the P-MP topology. Even if we try to provide on-demand fiber-optic link service, in which different remote antennas radiate different radio services, it is still possible to use conventional electrical multiplexing schemes such as frequency division multiplexing (FDM), time division multiplexing (TDM), or code division multiplexing (CDM) for the IF modulating signal, or an optical multiplexing scheme such as wavelength division multiplexing (WDM).

As described in Sect. 1 , fiber-optic links can be divided into the type based on intensity modulation/direct detection (IM/DD) and that based on optical remote heterodyne detection (RHD). The basic system configuration of these fiber-optic link techniques is illustrated in Figs. 2(a) and 2(b), respectively.

A fiber-optic link based on the IM/DD technique with with double side band (DSB) signal transmission especially has the simplest configuration as well as signal transparency. However it is well known that the IM/DD technique with DSB signal transmission suffers from a power penalty due to fiber chromatic dispersions [8] which increases as the transmitted radio frequency increases.

The paper [8] is demonstrating that the RF power $P_{f_{rf}}$ of the generated radio frequency transmitted by the IM/DD technique is vary approximately as

$$P_{f_{rf}} \propto \cos\left[\frac{\pi LD}{c}\lambda_c^2 f_{rf}^2\right], \tag{1}$$

where D is the dispersion parameter, L is the length of the fiber, and λ_c is the carrier wave length. This results in the occurrence of complete detected RF power cancellation for a fixed radio frequency f_{rf} at the fiber length of,

$$L = \frac{Nc}{2D\lambda_c^2 f_{rf}^2}, \qquad N = 1,3,5,\cdots. \tag{2}$$

For example, when we try to transmit 60 GHz radio signal with this technique, the RF power cancellation occurs at the fiber length of $1.02 \times N$ (N = 1,3,5, $\cdots$) [km], and when we try to transmit 65 GHz, that occurs at $0.87 \times N$ (N = 1,3,5,$\cdots$)[km].

Figure 3 shows the theoretical relationship between fiber length and normalized detected RF power when we transmit 60 GHz, 65 GHz, or 70 GHz RF carrier with the

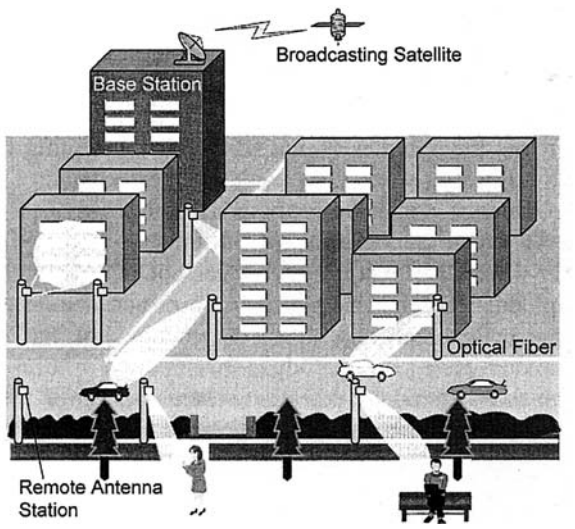

Fig.1 Concept of remote antenna systems based on fiber-optic links.

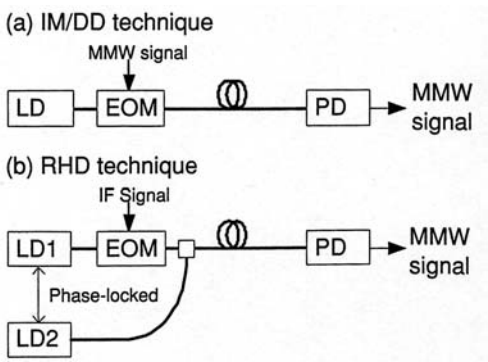

Fig.2 Basic system configuration of fiber-optic link.

IM/DD technique under the condition of the same received optical power. We can see from this figure that we need to carefully design the fiber-optic link considering the power penalty, which depends on RF frequency and fiber length, when we use the IM/DD Iink.

On the other hand, a fiber-optic link based on RHD including our proposed technique in this paper or single-sideband (SSB) signal transmission technique does not suffer from any power penalty in fiber-optic link in principle [8] . In addition, the RHD technique can also provides a frequency-conversion function and can easily generate a higher frequency.

Therefore, a fiber-optic link based on the RHD technique would seem to have greater potential for the near future. However, conventionally, it requires an expensive mode-locked dual-frequency laser transmitter or two laser transmitters with slightly different wavelengths, the phases of which must be strictly correlated. The strict phase correlation between two lasers can be achieved by using an optical phase-locked loop transmitter configuration, for example. However, this adds significantly to the complexity and cost of producing the optical transmitter, that is, the base station.

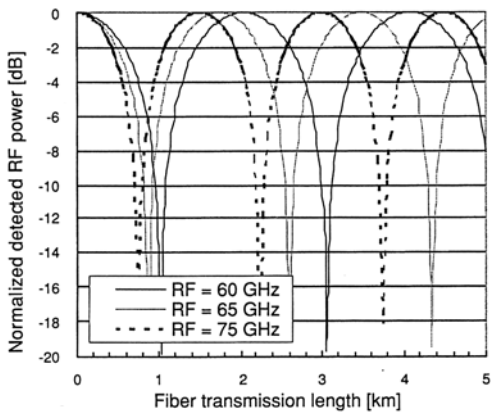

Fig.3 Power penalty due to chromatic fiber dispersion in IMDD.

3. System Configuration and Operating Principle

3. 1 Basic System Configuration

Figure 4 illustrates the basic system configuration of a broadband signal distribution link based on millimeter-wave self-heterodyne transmission/optical heterodyne detection. In this figure, the spectrum at each signal conversion stage are also shown to help illustrate the operating principle.

The basic components of the BS are two laser transmitters operating with a wavelength offset corresponding to the desired radio frequency, an external optical modulator to generate a single-side-band modulated signal with a residual carrier (SSB-EOM), an optical coupler, and an IF signal generator. Note that independent oscillation of the two lasers is allowed in this system, that is, we do not need an expensive, mode-locked dual-frequency laser or complicated phase-locked operation of the two laser transmitters.

One of the two optical carriers is modulated with the IF band signal using the SSB-EOM. As a result, an optical single-side-band modulated signal with a residual carrier is generated (see the spectrum at point-a). This optical signal is coupled with the other optical carrier with a wavelength offset corresponding to the desired millimeter-wave frequency using polarization maintaining fibers (PMF) and optical coupler, and transmitted to the RAS over fiber (see the spectrum at point-b).

Those optical signals are detected at the RAS using a photo-detector. As a result, a millimeter-wave band SSB-modulated signal with a residual carrier is obtained as shown in the spectrum at point-c in Fig. 4.

A millimeter-wave receiver, integrated in a mobile terminal such as a PC or PDA, can down-covert the received millimeter-wave signal by using a square-1aw detector because the transmitted signal is composed of a modulated signal and unmodulated carrier required for down-conversion. Furthermore, the frequency and phase of the obtained IF signal (see spectrum at point-d in Fig. 4) are extremely stable and independent of the frequency instability of the lasers in

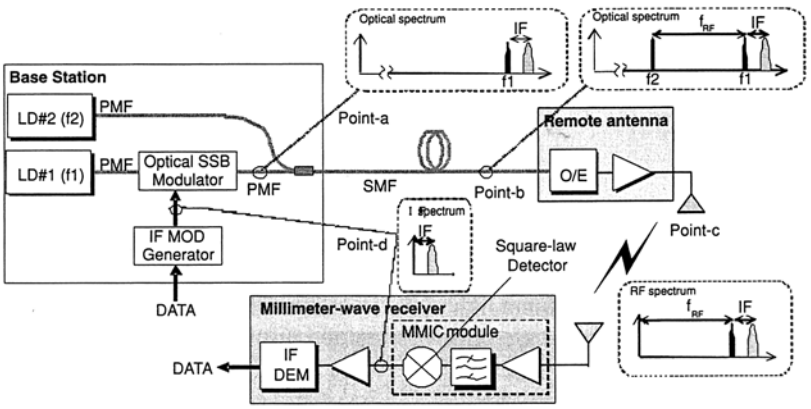

Fig.4 Basic system configuration of signal distribution link based on mmW self-heterodyne/optical heterodyne detection technique.

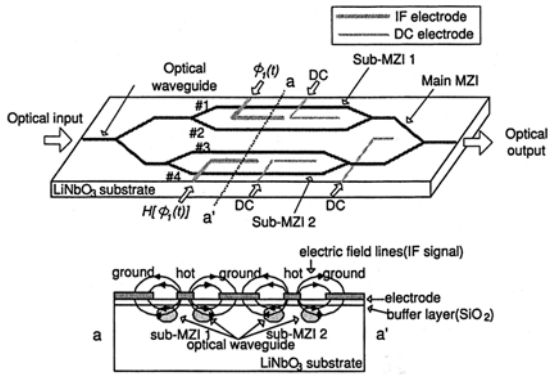

Fig.5 Basic configuration ot SSB-EOM.

the BS because the above up and down-conversion processes are based on self-heterodyne transmission. A more detailed explanation is provided in Sect. 3.2.

3.2 Principle of Millimeter-Wave Signal Generation for Self-Heterodyne Transmission and Detection

The SSB-EOM can be created using the well-known configuration of one Mach-Zhender interferometer (MZI) and two sub-MZIs on each of the main MZI arms, i.e., four parallel phase modulator waveguides [7]. The basic configuration of the SSB-EOM is shown in Fig. 5. The three MZIs (Main MZI, Sub-MZI1 , and Sub-MZI2) were fabricated on a commercial X-cut $LiNbO_3$ wafer using an ordinary Ti-diffusion technique. Each sub-MZI has a series of a co-planar IF and DC electrodes and the main MZI has a DC electrode to modulate the phase of the propagating optical field in the waveguides.

The propagating optical fields in the four parallel waveguides (#1–#2) are phase-modulated by IF signals as shown in Fig. 5 and the nth spectral component in each waveguide has an amplitude according to the Bessel function of the first kind, $J_n(m)$. in which m is the optical modulation index (OMI). When the IF signal is expressed by, $\phi(t) = V_m \cos \omega_{IF}t$, $\phi(t)$ and its Hilbert transformed signal, $H[\phi(t)]$, are simultaneously applied to both the two IF electrodes, the optical output of the SSB-EOM can be written as :

$$E_{1_{out}} = \frac{E_{1_{in}}}{2} e^{j[\omega_1 t+\theta_1(t)]} \cdot \left(e^{jm\cos\omega_{IF}t} + e^{jd_1}e^{-jm\cos\omega_{IF}t} + e^{jd_2}e^{jm\sin\omega_{IF}t} + e^{jd_3}e^{-jm\sin\omega_{IF}t}\right)$$

$$m = \frac{\pi}{2}\frac{V_m}{V_\pi} \quad (3)$$

where $E_{1_{in}}$, ω_1 , and $\theta_1(t)$ are the amplitude of the input lightwave, the optical angular frequency, and the phase-noise term of the optical carrier from the laser #1, respectively. d_1–d_3 are the respective static phase changes according to the level of DC voltage applied to each DC electrode. Some optical components generated in the waveguides #1–#4 are intensified in case they are coupled in phase at the waveguide junction points, while some are suppressed in case they are coupled out of phase. These conditions can be intentionally manipulated by tuning the values of m and d_1–d_3 .

The optical desired components, $J_0(m)$ and $J_1(m)$, are obtained after the manipulation, and the other components are suppressed to a sufficiently low level. Then, after the other optical carrier whose angle frequency is ω_2 is coupled, the ideal total optical signal in the fiber-optic link is expressed as,

$$E_{total} = E_1\left[J_0(m)e^{j[\omega_1 t+\theta_1(t)]} + J_1(m)e^{j[(\omega_1+\omega_{IF})t+\theta_1(t)]}\right] + E_2 e^{j[\omega_2 t+\theta_2(t)]}, \quad (4)$$

where E_1 and E_2 are respectively the output amplitude of the lightwave from laser #1 and laser #2 after each DC voltage, d_1–d_3, of the SSB-EOM is appropriately adjusted.

At the remote antenna station, the above optical signal is detected with a photo diode and directly converted to a millimeter-wave signal, and amplified with an RF amplifier. Since the photo diode operates as a square-law detector and the RF amplifier usually operates as a bandpass filter. As a result, the following SSB modulated RF signal with an unmodulated carrier, $s(t)$, is obtained.

$$\begin{aligned} s(t) &= BPF_{RF}\left\{\mathrm{Re}\left[E_{total}^2\right]\right\} \\ &= V_o\cos\left[\omega_{RF}+\omega_{IF}+\theta(t)\right]t \\ &\quad +\cos\left[\omega_{RF}+\theta(t)\right]t \end{aligned} \quad (5)$$

where $BPF_{RF}\{\cdot\}$ is a bandpass filtering operation for $\{\cdot\}$ in the RF band, which removes base-band signal and second and higher order frequency components. Re[·] is a real part of [·]. ω_{RF} is the RF frequency expressed by $\omega_{RF} = \omega_2 - \omega_1$ and $\theta(t)$ is the resultant total phase-noise component caused by heterodyning of the two optical lasers with an uncorrelated time-varying phase, expressed by $\theta(t) = \theta_2(t) - \theta_1(t)$. V_o is normalized RF modulated signal amplitude which is proportional to the product of $E_1J_1(m)$ and E_2 .

The millimeter-wave frequency band or channel obtained here can be selected simply by tuning the wavelength of laser #2. No matter which frequency band is selected, the millimeter-wave signal obtained after photo detection is composed of an unmodulated carrier and a single-side-band modulated signal with a frequency offset corresponding to that of the IF (see the RF spectrum at Point-c in Fig. 4). Use of this process for signal generation and frequency channel selection process make the RAS not only simple and low-cost, but also extremely flexible because it can handle any frequency band. keeping undesired signal components sufficiently suppressed without requiring millimeter-wave bandpass filter matching for the received frequency band.

The RF front-end for mobile terminals to receive transmitted millimeter-wave signals can be created using a low-cost circuit configuration because the received RF signals are down-converted to IF signals by a square-law detection technique without using a millimeter-wave local oscillator, as shown in Fig. 4. The square-law detection executes the

mixing of the received unmodulated carrier and SSB modulated signals expressed by Eq. (5). Adequate bandpass filtering operation in the IF band, BPF_{IF} [·] after the square-law detection regenerates the original IF modulated signal, $\phi(t)$, as follows.

$$\begin{aligned} r_d(t) &= BPF_{IF}\left[s^2(t)\right] \\ &= BPF_{IF}\left[V_o^2\frac{1+\cos 2\left[\omega_{RF}+\omega_{IF}+\theta(t)\right]t}{2}\right. \\ &\quad \left.+\frac{1+\cos 2\left[\omega_{RF}+\theta(t)\right]t}{2}+V_o\cos\omega_{IF}\right] \\ &= V_o\cos\omega_{IF} \end{aligned} \tag{6}$$

Considering V_o is proportional to $J_1(m)$ which is further approximately proportional to V_m in small m region, Eq. (6) shows $r_d(t)$ is approximately the exact IF transmitted signal, $\phi(t)$. As can be seen from Eq. (6), the regenerated IF signal is not disturbed at all by any phase-noise due to the lasers as a result of complete correlation of the phase-noise between both the unmodulated- carrier and SSB- modulated signal components.

4. Experimental Setup for Demonstration

Figure 6 illustrates the experimental setup we used and Table 1 lists some of the specifications of the experimental system.

We used two wavelength tunable laser transmitters with a 1.55μm wavelength band (TSL-210 manufactured by Santec Corporation). The laser transmitters had a frequency-lock option to maintain and stabilize the wavelength using an Eaton filter as the locking reference frequency. Consequently, once the frequency-lock function started operating, the frequency stability was about ±10 MHz.

To test the actual transmission performance for modulated signals, we used a 155.52-Mbps QPSK MODEM. A QPSK signal in the IF band with a 700-MHz center frequency was input into the IF input port of the SSB-EOM via a 90-degree hybrid. By adjusting the bias voltages for the three MZIs in the SSB-EOM, we obtained the desired optical SSB-modulated signal with a residual carrier while the undesired signal components were sufficiently suppressed. This signal was then coupled with the other optical carrier using polarization maintaining fibers and a 3-dB optical coupler and transmitted to a photo diode via a single-mode fiber.

The output millimeter-wave signal from the photo detector was first amplified and then connected to an RF front-end receiver module using WR 15 waveguides after providing some RF attenuation to simulate propagation loss. The

Tabte 1 Specifications ot experimental system.

Specifications of Base Stations	
Optical wavelength	1.55 μm band
Tunable laser	TSL-210 Santec Corp. with frequency lock option
Laser output power (typ)	10 mW for both lasers
Optical modulator	Optical SSB modulator (X-cut $LiNbO_3$)
Modulation	QPSK
Data	155.52 Mbps, PRBS:2^7-1
IF frequency	700 MHz
FEC (Forward Error Correction)	Not used
Detection method	Coherent detection
Specifications of Remote Antenna Station	
Transmitted RF frequency	59.2 GHz
Type of PD	UTC-PD (Bw=50 GHz)
Specifications of Millimeter-wave Receiver Module	
Operational frequency range	59–62 GHz (B_0=3 GHz)
Noise figure (F)	6 dB
Total receiver conversion gain	10 dB

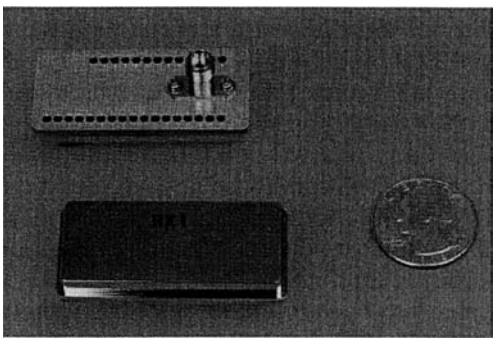

Fig.7 External appearance of millimeter-wave receiver module.

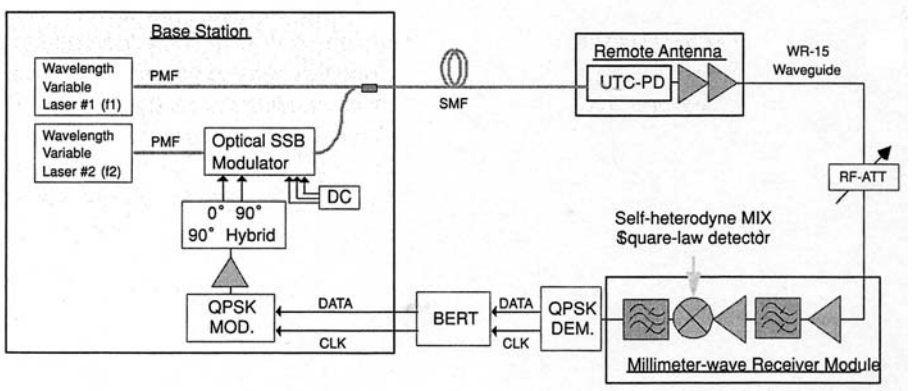

Fig.6 Experimental setup.

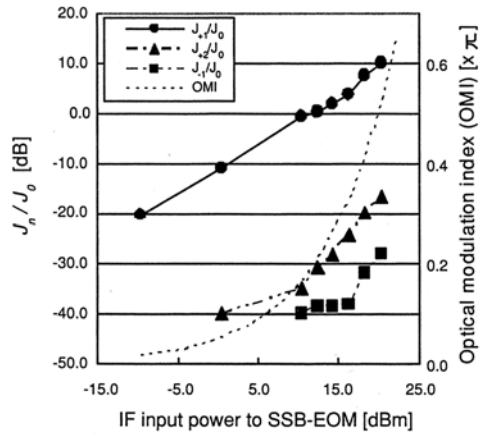

Fig.8 Desired and undesired spectrum component versus OMI.

RF front-end rec.eiver module was a down-converter module based on MMIC technology. The external appearance of the millimeter-wave receiver module is shown in Fig. 7.

The down-converted IF signal, which was obtained from the receiver module as an output, was demodulated using a QPSK demodulator. The demodulated data was used to evaluate the BER performance using a BER tester as shown in Fig. 6.

5. Experimental Demonstration

5.1 Spectrum of Generated Millimeter-Wave Signals

Figure 8 shows the relationship between the IF input power to the SSB-EOM and the power of their carrier component J_{+1} corresponding to the desired RF modulated signal, and the undesired carrier components J_{-1} and J_{+2}. The power of each carrier component was normalized by the power of the carrier component J_0 corresponding to the desired unmodulated RF carrier. This figure also shows the relationship between the IF input power and optical modulation index (OMI).

Figures 9 to 11 show the RF spectrum when the OMI was set to 0.075, 0.19, and 0.6π, respectively. As the figures show, the balance of the signal power between the desired unmodulated RF component J_0 and modulated RF signal component J_{+1}, and the signal suppression level of undesired components such as J_{-1} or J_{+2} varied according to the value of the OMI.

It has previously been reported that the best received CNR is obtained at a receiver module output when the received unmodulated carrier power J_0 equals the received RF modulated signal power J_1 when the total RF transmission power is limited [6].

As shown in the above results, by adjusting each bias voltage and setting the OMI to 0.19π, we succeeded in obtaining the desired RF spectrum, as shown in Fig. 10 where the power level of J_0 equals that of J_1 and the other undesired components were suppressed to a level of less than –30 dBc.

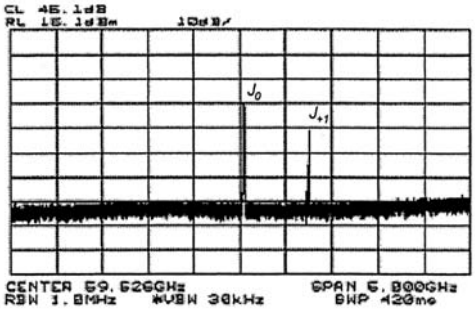

Fig.9 RF spectrum for OMI = 0.075π.

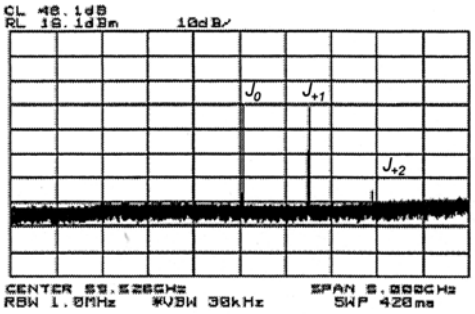

Fig.10 RF spectrum for OMI = 0.19π.

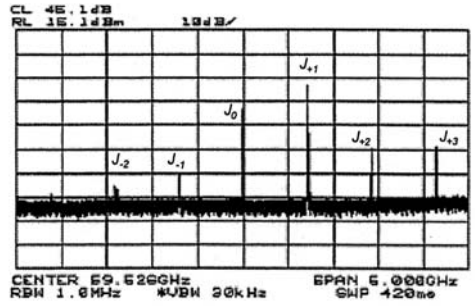

Fig.11 RF spectrum for OMI = 0.67π.

Reducing the power of J_{+2} and other undesired frequency components is a very important issue for our system because it is directly converted into spurious power out of the signal band or may be converted in co-channel interference as a result of the cross product between J_{+1} and J_{+2}.

In our experimental setup, we used an EOM using a well-known type of SSB configuration as described in [7]. As long as we try to generate an optical SSB modulated signal with residual carrier component by using this type of optical modulator, the generation of the J_{+2} component, specifically even harmonics of the desired frequency components, is theoretically inevitable. We however showed that it is possible to suppress the power of J_{+2} and other undesired components to less than –30 dBc in the experiment by appropriately carefully adjusting each bias voltage that drives DC electrode.

The value of less than –30 dBc Seems to be sufficiently small from the viewpoint of Japanese radio regulations for the 60 GHz unlicensed band, and also from the viewpoint of

acceptable power of interference.

Now, we assume the RF transmission power of 10 dBm referring to the upper limitation restricted by the Japanese radio regulation for 60 GHz unlicensed band, and also assume that approximately 7 dBm of RF power is distributed for local power and the rest (7 dBm) is for signal power because this power distribution is known to be the optimum one to obtain the maximum carrier-to-noise power ratio (CNR) performance.

Under these assumptions, the undesired J_{+2} component power of –30 dBc generates –23 dBm of spurious power out of the signal band. According to the Japanese regulation, this spurious must be less than –10 dBm. Therefore the J_{+2} component power of –30 dBc is sufficiently small from the viewpoint of Japanese radio regulations.

On the other hand, the J_{+2} component's power level is such that it may cause a signal-to-interference power ratio (CIR) performance degradation of 30 dB . However, this CIR level is high enough considering that the required CNR performance is generally around 15–20 dB , although it depends on the modulation format used. Thus, the J_{+2} component's power level is also sufficiently small from the viewpoint of acceptable power of interference.

5.2 Cancellation of Frequency Instability

As described in Sect. 3, the transmitted RF signal is composed of an unmodulated RF carrier and an SSB-modulated RF signal. Since they are generated by heterodyning of two optical carriers, which are transmitted from independently oscillating laser transmitters, they both have severe frequency instability. However, this instability is completely canceled out at the receiver module according to the principle of millimeter-wave self-heterodyne transmission.

Figure 12 shows the magnified transmitted RF spectrum of J_0 when OMI was 0.19π, which gives the optimum RF spectrum as shown in Fig. 10. As Fig. 12 shows, frequency instability of over 10 MHz was measured, though the appearance of the spectrum depended on the sweep-time, the observation time, and other display setting of the spectrum analyzer.

Figure 13 shows the spectrum of the IF signal obtained by detecting the received RF signal with a receiver module. As the figure shows, an extremely stable IF carrier was obtained after self-heterodyne detection at the receiver module, and frequency instability was successfully canceled oul in comparison to the received RF spectrum in Fig. 12.

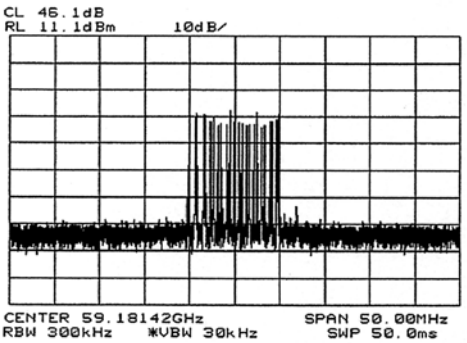

Fig.12 RF spectrum in unmodulated IF carrier transmission.

5.3 Received CNR Performance

Figure 14 shows the relationship between the received RF power at a receiver module and the CNR performance of the detected IF signal when the optical fiber length was 2 m, 5 km, and 10km, respectively. In this figure, we also show the received CNR performance, which was theoretically calculated neglecting the signal degradation in the optical link, The theoretical received CNR when the millimeter-wave self-heterodyne transmission technique was used is given by the following equation [6],

$$CNR = \frac{P_r^2}{8B\left[B_0(kTF)^2 + P_r kTF\right]} \tag{7}$$

where P_r is the total received RF power, B is the signal bandwidth, and B_0 is the noise bandwidth input to the square-law detector (effective operational frequency range for square-law detection). In calculating the theoretical CNR performance. we used the value of B_0 = 3.0 GHz because the 3-dB bandwidth of the bandpass filter in the receiver module was about 3 GHz.

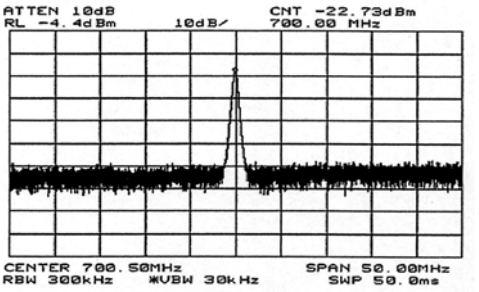

Fig.13 Spectrum of detected IF carrier.

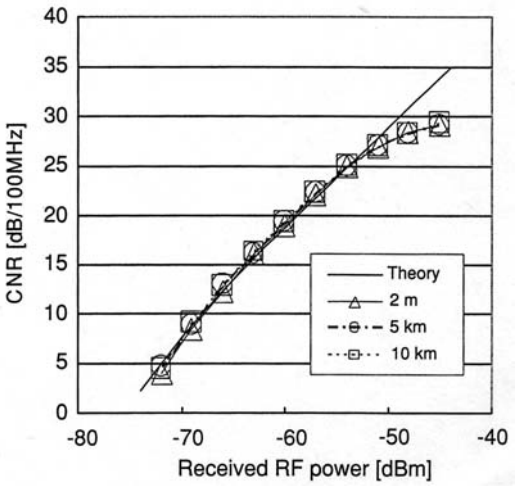

Fig.14 CNR performance versus received RF power (BW = 100 MHz).

Table 2 Link budget design for RF link.

RF transmission power	10 dBm
Antenna gain	Tx:6 dBi, Rx:6 dBi
RF frequency	59.2 GHz
Distance D	5 m
Propagation loss (given by $(4\pi D/\lambda)^2$)	82 dB
Received RF power	10 − 82 + 6 + 6 = −60 dBm

As can be seen from Fig. 14, the received CNR performance did not depend on the fiber length at all, and the value was almost equal to the theoretical value when the received RF power was less than about –55 dBm. This means the total CNR performance including the both the fiber-optic and RF links, was dominated by that of the RF link under our experimental condition.

When the received RF power was more than –60 dBm, the received CNR performance was suppressed because the amplifier and mixer in the receiver module were saturated.

As Fig. 14 shows, a received CNR of more than 18 dB/100 MHz Was obtained when the received RF power was –60 dBm. We can translate this result to mean that we could transmit a 100-MHz bandwidth signal over 5 m with a received CNR of more than 18 dB if we assume an RF transmission power of 10 mW and the use of 6-dBi antennas for both the transmitter and receiver. Table 2 lists the link budget design for the RF link required for this scenario.

Please note here that the link budget design of Table 2 is not taking into consideration the multipath effect. We actually need to consider it when we use a broad beam-width transmitter and receiver antennas with low antenna gain. Thus we have studied a technique to overcome the signal fading caused by multipath affecting millimeter-wave signal transmission [9].

Fortunately the radio signal format obtained with our technique, that is, signal type for self-heterodyne detection enables us to use a simple integrated antenna diversity receiver [9]. In addition, it has been reported in [9] that the use of orthogonal frequency division multiplexing (OFDM) format modulation combined with the integrated antenna diversity receiver can greatly improve the receiver-sensitivity and that it overcomes serious signal fading without using expensive or complicated technologies.

However discussing or describing the details of the technique is beyond the scope of this paper and we therefore do not take into consideration multipath effect in our link budget design in this paper.

5.4 BER Performance in 156-Mbps QPSK Signal Transmission

Figure 15 shows the relationship between the received RF power at a receiver module and the BER performance for various optical fiber lengths when the received optical power at the photo receiver was –2.6 dBm and the OMI was set to 0.19π.

As Fig. 15 shows, the BER performance did not depend on the fiber length at all, as was the case for the received

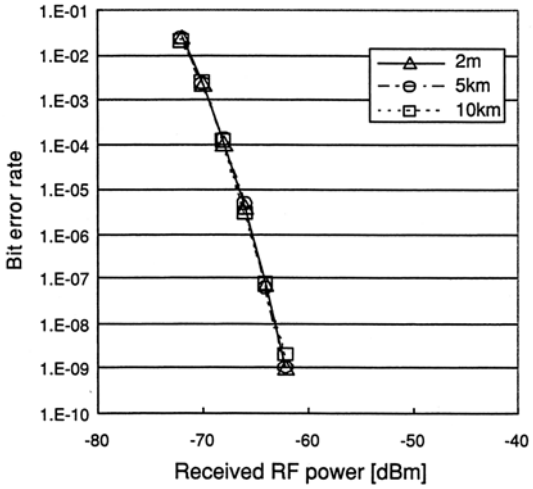

Fig.15 BER performances versus received RF power for 156 Mbps QPSK signal transmission test.

CNR performance. Error-free performance was obtained when the received RF power was more than –62 dBm. We can translate this results to mean that a 156-Mbps QPSK signal could be transmitted error free over 5 m if we assume a transmission power of 10 mW and the use of 6-dBi antennas for the transmitter and receiver, as explained in Sect. 5.3.

A BER of 10^{-5} would probably be sufficient in an actual system because forward error correction is usually used. In this case, we can read from Fig. 15 that the allowable received RF power is less than –66 dBm. We can again translate this result to mean that it would be possible to extend the transmission distance in Table 2 to 10 m since the propagation loss would increase by 6 dB if the distance was doubled.

5.5 Discussion about Frequency Stability Required to Lasers

We used two frequency-stable tunable laser transmitters with a frequency-locked option in our experimental demonstration because this was our first experiment to demonstrate our proposed technique, which uses two free running lasers and does not use an optical PLL, enables frequency-offset free and phase-noise free signal transmission.

From the operational viewpoint, our technique does not require such an expensive function to stabilize the laser frequency unless the obtained radio frequency deviates out of the operational band of the millimeter-wave receiver module.

As a practical matter, the radio regulation usually limits the maximum frequency deviation allowed for the frequency band or the wireless system. Therefore it is supposed that we usually need to stabilize optical laser's frequency to some extent. However, it is clear that a BS which requires an optical PLL is more complex than a BS which requires a function just to stabilize each laser's frequency to some extent.

Furthermore even if our system uses an optical PLL at the BS, our system still has a great advantage compared to the conventional RHD technique. The frequency stability or

phase-noise performance of the radio signal obtained at remote antenna stations fundamentally depends on perfectibility of the operation of optical PLL used in the BS when the conventional RHD technique is used. However it is usually difficult or expensive to create an optical PLL that realizes perfect phase correlation between two lasers.

On the other hand, our technique enables perfect phase-noise free and frequency-offset free signal transmission in principle, and these effects are easily obtained independently of if optical PLL is used or not.

In addition, our technique, which does not need an optical PLL, has a great possibility in that we can install local laser (laser #1) at remote antenna station for heterodyne detection, though it was not discussed in detail in this paper. We hope this configuration can bring about an improvement in performance.

6. Conclusion

We proposed a fiber-optic broadband millimeter-wave signal distribution link based on a millimeter-wave self-heterodyne transmission technique over an optical heterodyne detection technique. We theoretically and experimentally showed that the proposed fiber-optic link is not disturbed by the frequency instability of the laser and is capable of distributing broadband millimeter-wave signals without using requiring a complicated and expensive laser transmitter such as a dual-mode-locked laser or an optical phase locked loop laser, while offering the advantages of optical remote heterodyne detection. We experimentally demonstrated that the proposed fiber-optic millimeter-wave link could successfully transmit a 156-Mb/s QPSK-formatted signal over a 10-km fiber link and a 5-m pseudo-air link with bit-error-free performance, or over a fiber link and 10-m pseudo-air link with a BER of 10^{-5}.

References

[1] G. Grosskopf, R. Eggermann, S. Zinal, B. Kuhlow, G. Przyrembel, D. Rohde, A. Korke, and H. Ehlers, "Photonic 60-GHz maximum directivity beam former for smart antennas in mobile broad-band communications," IEEE Photonics Technol. Lett., vol. 14, no.8, pp. 1169–1171, Aug. 2002

[2] H. Yamamoto, K. Hase, K. Utsumi, M. Miyashita, M. Kurono, Y. Serizawa, Y. Shoji, and H. Ogawa, "Development of gigabit millimeter-wave broadband wireless access system remote antenna systems incorporating radio-over-fiber and coarse-WDM," Proc. APMC'03, vol.2, pp.965–968, Nov. 2003.

[3] U. Gliese, T.N. Nielsen, S. Norskov, and K.E. Stubkjaer, "Multifunctional fiber-optic microwave links based on remote heterodyne detection," IEEE Trans. Microw. Theory Tech., vol.46, no.5, pp.458–468, May 1998.

[4] M. Ogusu, K. Inagaki, and Y. Mizuguchi, "60-GHz-band millimeter-wave generation using two-mode injection locking of Fabry-Perot laser," IEICE Technical Report, MW99-32, OPE99-16, June 1999.

[5] H. Ito, F. Nakajima, T. Furuta, K. Koshino, Y. Hirota, and T. Ishibashi, "Photonic terahertz-wave generation using antenna-integrated uni-travelings-carrier photodiode," Electron. Lett., vol.39, no.25, pp. 1828–1829, Dec. 2003.

[6] Y. Shoji, K. Hamaguchi, and H. Ogawa, "Millimeter-wave remote self-heterodyne system for extremely stable and low-cost broadband signal transmission," IEEE Trans. Microw. Theory Tech., vol.50, no.6, pp. 1458–1468, June 2002.

[7] M. Izutsu, S. Shikama, and T. Sueta, "Integrated optical SSB modulator/frequency shifter," IEEE J. Quantum Electron., Vol.QE- 17, no.11, pp.2225–2227, Nov. 1981 .

[8] G.H. Smith, D. Novak, and Z. Ahmed, "Overcoming chromatic-dipersion effects in fiber-wireless systems incorporating external modulators," IEEE Trans. Microw. Theory Tech., vol.45, no.8, pp.1410–1415, Aug. 1997.

[9] Y. Shoji and H. Ogawa, "70-GHz-band MMIC transceiver with integrated antenna diversity system: Application of receiver-module-arrayed self-heterodyne technique," IEEE Trans. Microw. Theory Tech., vol.52, no.11, pp.2541–2549, Nov. 2004.

Yozo Shoji received the B.E. and M.E. degrees in electrical engineering and Dr. Eng. degree in communications engineering from Osaka University, Osaka, Japan, in 1995, 1996, and 1999, respectively. In 1999, he joined the Yokosuka Radio Communications Research Center, Communications Research Laboratory (CRL), Ministry of Post and Telecommunications, Kanagawa, Japan, as a Researcher. He is currently a Researcher with the National Institute of Information and Communications Technology (NICT), Incorporated Administrative Agency, Kanagawa, Japan, where he has been engaged in research on millimeter-wave communications system and millimeter-wave/microwave photonics system. He was the recipient of the 2000 IEICE Science Promotion Award and the 2003 CRL Excellent Achievement Award for his invention of the millimeter-wave self-heterodyne transmission technique.

Yoshihiro Hashimoto received the B.E. degree in electronics and communications and M.E. degree in electrical engineering from Meiji University, Tokyo, Japan, in 1995 and 1997, respectively. In 1997, he joined Opto-electronics Research Division, New Technology Research Laboratories, Sumitomo Osaka Cement Co., Ltd., Chiba, Japan. He has been engaged in research and development of optical modulators.

Hiroyo Ogawa received the B.S., M.S., and Dr. Eng. degrees in electrical engineering from Hokkaido University, Sapporo, in 1974, 1976, and 1983, respectively. He joined the Yokosuka Electrical Communication Laboratories, Nippon Telegraph and Telephone Public Corporation, Yokosuka, in 1976. He has been engaged in the research and development on microwave and millimeter-wave integrated circuits, monolithic integrated circuits, and subscriber radio systems. From 1990 to 1992, he was engaged in the research of optical/microwave monolithic integrated circuits and fiber optic links for millimeter-wave personal communication systems at ATR Optical and Radio Communication Research Laboratories. From 1993 to 1998, he was engaged in microwave photonics and microwave and millimeter-wave signal processing techniques for communication satellites at NTT Wireless Systems Laboratories. In July 1998 he joined the Communication Research Laboratory, Ministry of Posts and Telecommunications, and he has been researching, developing and standardizing millimeter-wave wireless access systems. He is currently working at National Institute of Information and Communications Technology and conducting Millimeter-Wave Promotion Project at Yokosnka Radio Cornmunication Research Center. Dr. Ogawa served on the IEEE MTT-S Symposium Technical Conmttee and was a member of the MTT-S Technical Committee and MWP Steering Committee. He also served on Editorial Committee of IEICE Trans. on Electronics as an associate editor in 1990–1992, MTT-Tokyo Chapter as a secretary/treasurer in 1991–1992, IEICE Microwave Technical Group as a secretary in 1993–1994 and a vice-chair in 1999–2002, IEICE Microwave Photonics Technicai Group as a secretary in 1995–1998, a vice-chair in 1999–2000, and a chair in 2001–2002, the 1996 Intemational Topical Meeting on Microwave Photonics (MWP96) as a secretary and MWP2002 as a finance chair. He also chaired the Technical Program Cornmittee of 1998 Asia-Pacific Microwave Conference (APMC98), the Steering Committee of Microwave Workshop & Exhibition (MWE2003) and served on the Steering Committee of APMC2002 as a vice-chair. He has served on TSMMW (Topical Symposium on Millimeter Waves) Committee as a secretary since 1999. He is a member of IEEE.